

Simulation of Flux Lines with Columnar Pins: Bose Glass and Entangled Liquids

Prasenjit Sen¹, Nandini Trivedi^{1*} and D. M. Ceperley²

¹ *Department of Theoretical Physics, Tata Institute of Fundamental Research, Homi Bhabha Road, Mumbai 400005, India*

² *Department of Physics and National Center for Supercomputing Applications, University of Illinois at Urbana-Champaign, Urbana, Illinois, 61801, USA.*

Using path integral Monte Carlo we simulate a 3D system of up to 1000 magnetic flux lines by mapping it onto a system of interacting bosons in (2+1)D. With increasing temperature we find a first order melting of flux lines from an ordered solid to an entangled liquid signalled by a finite entropy jump and sharp discontinuities in the defect density and the structure factor $S(\mathbf{G})$ at the first reciprocal lattice vector. In the presence of a small number of strong columnar pins, we find that the crystal is transformed into a Bose glass phase with patches of crystalline order nucleated around the trapped vortices but with no overall positional or orientational order. This glassy phase melts into a defected entangled liquid through a continuous transition.

PACS numbers: 74.60.-w, 74.60.Ge, 72.25.Dw, 05.30.-d, 05.10.Ln

(November 20, 2018)

The seminal paper of Abrikosov in 1957 [1] showed, within a mean field calculation, that for fields below a critical field $H_{c2}(T)$ a type II superconductor allows magnetic flux to penetrate in the form of a triangular array of vortices each carrying a unit flux quantum $\phi_0 = hc/2e$. This picture is modified considerably in the case of high T_c cuprates which are quasi two-dimensional and have high transition temperatures [2]. The most dramatic consequence of the enhanced thermal fluctuations on the Abrikosov lattice is its melting into a vortex liquid by a first order transition as indicated in resistivity, neutron scattering, specific heat, SQUID magnetometry and local Hall probe [3] measurements. Peak effect [4] measurements on NbSe₂ have also found a reentrant phase diagram in the H-T plane [5,6]. Theoretical calculations have primarily been confined to density functional approaches on the layered system of pancake vortices [7] valid for BSCCO, lattice simulations of frustrated 3D XY-models [8], Monte Carlo or Langevin dynamics of the vortices [9], and determination of the melting line using Lindemann criterion [10]. Simulations of vortices, treated as line or polymer-like objects, have been done using an analogy with interacting bosons [5] by variational and path integral techniques [6,11].

The effect of pins on the structure and dynamics of the vortex lattice adds another dimension to vortex behavior. The original work of Larkin and Ovchinnikov [12] predicted that for $d < 4$, point pins destroy the long range order of the vortex lattice and break it up into small ordered coherence volumes. From the point of view of practical applications where the aim is to minimize the motion of vortices in order to reduce dissipation, it is found that columnar pins along the vortex direction are extremely effective in pinning vortices [13]. There have been very few simulations attempting to study the phases and phase transitions in the presence of columnar pins. The ones based on 3D XY models assume an underlying

numerical grid which affects the vortex structures for the small system sizes and high vortex densities that have been studied [14,8].

With this motivation, in this Letter we present the first simulations of the structure and thermodynamics of up to 1000 vortices with and without strong columnar pins using a *continuum* path integral quantum Monte Carlo (PIMC) simulation of the corresponding interacting bosons in (2+1)D. There is no bias of a superimposed lattice and no prior input of the nature of wave functions or the type of the transition. We extend previous simulations [11] to include columnar pins on considerably larger lattices.

Our main findings are as follows— In the pure system, we see the reentrant nature of the melting line in agreement with the predictions of Nelson [5]. We find a triangular solid phase at low temperatures T which melts into an *entangled* liquid phase at higher T by a first order transition with a finite entropy jump. The defect density, and structure factor at the first reciprocal lattice vector, $S(\mathbf{G})$, also show sharp discontinuities at the transition. In the solid phase, $S(\mathbf{G}) \sim \mathcal{O}(N)$ and drops sharply to $\mathcal{O}(1)$ in the liquid phase. In the presence of 10% columnar pins, the vortex lattice transforms into a Bose glass phase at low T . The Bose glass consists of patches of ordered regions with only short range positional *and* orientational order. This phase is qualitatively different from the Bragg glass phase with point pins [15]. With increasing temperature, there is a transition from a Bose glass to an entangled ‘defected liquid’ which is considerably smeared.

Consider a system of N flux lines in 3D characterized by a bending energy $\tilde{\epsilon}_1 = \{\phi_0/(4\pi\lambda)\}^2$ [16] where λ is the London penetration depth. The inter-vortex interaction is approximated as $V(r_{ij}) = \epsilon_0 K_0(r_{ij}/\lambda)$ where $\epsilon_0 = \phi_0^2/(8\pi^2\lambda^2)$ is the scale of the inter-vortex potential, K_0 is the modified Bessel function of the first kind and $\mathbf{r}_i(z)$'s

are the 2D position vectors of the flux lines in a plane perpendicular to their length at a height z . $K_0(r) \sim -\ln(r)$ as $r \rightarrow 0$ and is valid in the high vortex density limit, the regime studied in Ref. [11]. In this paper, we fix the density on the lower part of the reentrant melting curve [6] and therefore retain the full $K_0(r)$ form of the potential.

The partition function of the flux lines is mapped onto the world lines or Feynman paths of bosons [5] described by the Hamiltonian

$$H = -\Lambda^2 \sum_{i=1}^N \nabla_i^2 + \sum_{i<j} K_0(r_{ij}) \quad (1)$$

The bosonic path integrals are in two spatial dimensions and one imaginary time direction, which is equivalent to the thickness of the sample along the direction of the magnetic field. All lengths are measured in units of λ and energies in units of ϵ_0 . The dimensionless de Boer parameter $\Lambda = k_B T / (2\tilde{\epsilon}_1 \lambda^2 \epsilon_0)^{1/2}$ is a measure of quantum fluctuations (the relative strength of the kinetic energy *vs* the interaction energy) of the boson system, or equivalently a measure of temperature T in the vortex system. Once the mapping is established, we do a PIMC simulation [17] of interacting bosons at an inverse boson temperature $\beta = 1/T_b$ [18]. Periodic boundary conditions are used in all directions and permutations between bosons are included [19]. If $T_b < \Lambda^2 \rho$, where $\rho = N\lambda^2 / (\text{Area})$ is the dimensionless density of the bosons, exchanges between the particles are possible and can generate entangled vortex lines.

In Fig. 1(a) we show the structure of 1000 vortices at low temperature $\Lambda = 0.045$ where the vortex system shows a beautiful triangular lattice with small excursions of the vortex lines about their equilibrium positions seen in Fig. 2(a). For $\Lambda > 0.064$ the vortices melt into an entangled liquid as seen from the actual configurations of the vortex lines in Fig. 2(b). Concomitantly, the superfluid density ρ_s of the corresponding boson system jumps from zero in the solid phase to a finite value in the liquid phase. The entanglement correlation length [5], which is the typical length along the z -direction for vortex lines to cross, is on the order of the sample size in the solid and drops to $\sim 4a_0$, where a_0 is the planar lattice constant, in the liquid phase.

The degree of positional order is quantified by the structure factor $S(\mathbf{k} = \mathbf{G})$ at the first reciprocal lattice vector of the triangular lattice. As seen in Fig. 3, with increasing temperature there is a sharp transition from a crystalline to a liquid phase at $\Lambda_m \sim 0.064$. In a temperature-driven first order transition, the free energy is continuous across the transition but the internal energy and entropy are discontinuous. In analogy in the mapped boson problem at $T = 0$, the total energy is continuous but there are sharp jumps in the potential and kinetic energies between $\Lambda = 0.062$ and 0.064 . The melting transition is located by the intersection of the poly-

nomial fits to the energy in the liquid and solid phases at $\Lambda_m = 0.064$ in good agreement with Ref. [6].

In the crystal $S(\mathbf{k})$ shows Bragg peaks with $S(\mathbf{G}) \sim \mathcal{O}(N)$, where N is the number of vortices, while above Λ_m , $S(\mathbf{k})$ is liquid-like with $S(\mathbf{G}) \sim \mathcal{O}(1)$. By fitting the structure factor data to the form $S(\mathbf{G}) = 1 + (N - 1) \exp(-G^2 \langle u^2 \rangle)$ for a finite system we have calculated the Lindemann number $c_L = \langle u^2 \rangle^{1/2} / a_0 = 0.24$ at the transition just within the solid phase, in good agreement with other works [2], where $\langle u^2 \rangle$ is the mean squared displacement of the particles from their lattice positions [20].

In addition to the positional correlations, the orientational order for six-fold symmetry is described by $\Psi_6(\mathbf{r}_i) = (1/6) \sum_j e^{i6\theta_{ij}}$, where the sum over j runs over all the nearest neighbors of i in a triangulation picture, and θ_{ij} is the angle the bond between particles at \mathbf{r}_i and \mathbf{r}_j makes with an arbitrary reference axis. The orientational correlation function defined as $g_6(r) = \langle \Psi_6(r) \Psi_6^*(0) \rangle$ also shows long range order in the clean system at low T . We find that the correlation lengths for positional and orientational order can reliably be extracted only from data on large system sizes ~ 1000 vortices and we find that both types of order vanish at Λ_m .

A measure of imperfections in the triangular arrangement of the flux lines is the number of topologically-defected non six-fold coordinated sites in the Delaunay triangulation [21] of imaginary time slices of the system. This defect density is small at low temperatures in the clean system and shows a sharp jump across the melting transition (Fig. 4).

Effect of Columnar Pins:

In the boson picture, randomly placed potential wells are correlated in the imaginary-time direction and correspond to columnar pins in the vortex representation. We model the columnar pin as an attractive delta function which traps a vortex all along its length. In the boson picture the trapped vortex corresponds to a fixed classical particle. The vortex phase in the presence of columnar pins has been previously referred to as a Bose glass phase [5]. Our simulations provide the first detailed description of the structure and properties of this so-called Bose glass. In Fig. 1(b) we show the configuration of the 1000 vortex system at $\Lambda = 0.045$ with 10% of the vortices, those trapped by columnar pins, held fixed. The pins are found to seed or nucleate an ordered crystalline patch, however, since the pins are randomly located, the different patch orientations are not commensurate and frustrates the translational and orientational order of the lattice. Columnar pinning dramatically reduces $S(\mathbf{G})$ from around 250 in the pure 1000 vortex system to about 6 in the presence of pins at $\Lambda = 0.045$ in the Bose glass phase (Fig. 5(a)). In addition, $S(k)$ has a jagged peak, with shoulders and split peaks, which are characteristic of glasses. The Bose glass is rather different from a structural glass or a frozen liquid which has a peak height of $S(\mathbf{G}) \approx 1.5$. At higher temperatures

the Bose glass melts into a defected liquid phase where the unpinned vortices are entangled (Fig. 2(c)). In the parameter region investigated, we do not find any evidence for a disentangled liquid either with or without pins. The Bose glass phase that we find in these simulations is in a different limit from that studied by Nelson and Vinokur [22] where the number of columnar pins is much larger than the number of vortices.

The topological defects generated by the columnar pins in the vortex lattice destroy the positional and orientational order within few lattice spacings (Fig. 5(b)) in contrast to a Bragg glass [15] in the presence of weak point pins which retains long range orientational order and algebraic positional order.

Columnar pinning has a marked effect on the first order melting transition. The kinetic and potential energies vary smoothly through the transition. The sharp drop in $S(\mathbf{G})$ in Fig. 3 also disappears. The sharp jump in defect density is replaced by a much smoother increase through the transition as seen in Fig. 4. The local variations in the melting temperature caused by the quenched random potential below a certain critical dimension can cause a sharp first order transition to get rounded off in presence of quenched randomness [23]. It is possible that at lower pin densities, the first order jumps in various quantities persist with reduced magnitudes. Further simulations are in progress to study the evolution of the sharp first order transition with increasing defect density.

P. Sen would like to acknowledge B. Militzer, G. Bauer and E. Draeger for help with the code. We would also like to thank S. Banerjee, S. Bhattacharya, C. Dasgupta, T. Giamarchi, A. Grover, G. Menon, and A. Paramekanti for useful discussions. We acknowledge the support of the NCSA, UIUC for computational resources and software and the NSF grant no. DMR 98-02373.

* e-mail: ntrivedi@tifr.res.in

-
- [1] A. A. Abrikosov, Sov. Phys. JETP **5**, 1174 (1957).
 - [2] G. Blatter et. al., Rev. Mod. Phys. **66**, 1125 (1994).
 - [3] H. Safar et. al. Phys. Rev. Lett. **69**, 824 (1992); R. Cubitt et. al. Nature **365**, 407 (1993); U. Welp et. al. Phys. Rev. Lett. **76**, 4809 (1996); E. Zeldov et. al. Nature **375**, 373 (1995); A. Schilling et. al. Nature **382**, 791 (1996);
 - [4] K. Ghosh et. al. Phys. Rev. Lett. **76** 4600 (1996).
 - [5] D. R. Nelson, Phys. Rev. Lett. **60**, 1973 (1988); D. R. Nelson and H. S. Seung, Phys. Rev. B **39**, 9153 (1989).
 - [6] W. R. Magro and D. M. Ceperley, Phys. Rev. B **48**, 411 (1993).
 - [7] S. Sengupta et. al. Phys. Rev. Lett. **67**, 1023 (1991).
 - [8] (a) R. E. Hetzel et. al. Phys. Rev. Lett. **69**, 518 (1992); (b) Y. Li and S. Teitel, Phys. Rev. B **47**, 359 (1993) and **49**, 4136 (1994); (c) A. E. Koshelev, Phys. Rev. B **56**, 11 201 (1997); (d) S. Ryu and D. Stroud, Phys. Rev. Lett. **78**, 4629 (1997); (e) X. Hu, S. Miyashita and M. Tachiki *ibid.* **79**, 3498 (1997).
 - [9] S. Ryu et. al. Phys. Rev. Lett. **68**, 710 (1992); S. Ryu

- and D. Stroud, Phys. Rev. B **54**, 1320 (1996); Otterlo et. al. Phys. Rev. Lett. **84**, 2493 (2000).
- [10] A. Houghton, R. A. Pelcovits, and A. Sudbo, Phys. Rev. B **40** 6763 (1989); G. Blatter and H. Nordborg, Phys. Rev. B **54**, 72 (1996).
- [11] H. Nordborg and G. Blatter, Phys. Rev. Lett. **79**, 1925 (1997); Phys. Rev. B **58**, 14556 (1998).
- [12] A. I. Larkin and Yu. V. Ovchinnikov, J. Low Temp. Phys. **34**, 409 (1979).
- [13] L. Civale et. al. Phys. Rev. Lett. **67**, 648 (1991); Ch. Simon et. al. Nucl. Instr. and Meth. in Phys. Res. B **107**, 384 (1996); G. Pasquini et. al. Physica C **274**, 165 (1997).
- [14] K. H. Lee, D. Stroud and S. M. Girvin, Phys. Rev. B **48**, 1233 (1993).
- [15] T. Giamarchi and P. Le Doussal, Phys. Rev. B **52** 1242 (1995).
- [16] D. R. Nelson in *The Los Alamos Symp. 1991, Applications of High-temperature Superconductors*, Ed: K. S. Bedell et. al. (Addison-Wesley Pub. Co. 1992).
- [17] D. M. Ceperley, Rev. Mod. Phys. **67**, 279 (1995).
- [18] We use $\beta = 1/T_b = 20000$ which is discretized into $M = 128$ slices. The time step $\delta\tau \equiv \beta/M = 156.25$ and the typical energy $E \sim 10^{-3}$, which ensures that the Trotter error $\delta\tau E \ll 1$.
- [19] It is possible to have an entangled liquid with either bosons or boltzmannons, but bosons generate the $T_b = 0$ state at a higher temperature and are thus computationally more convenient [17].
- [20] The mean squared displacement $\langle u^2 \rangle$ can also have some finite size effects, see E. Draeger and D. M. Ceperley, Phys. Rev. B **61** 12094 (2000).
- [21] F. F. Preparata and M. L. Shamos, *Computational Geometry: An Introduction*, (Springer-Verlag, New York, 1985).
- [22] D. R. Nelson and V. M. Vinokur, Phys. Rev. B **48** 13060 (1993).
- [23] Y. Imry and M. Wortis, Phys. Rev. B **19** 3580 (1979).

FIGURE CAPTIONS

FIG. 1. Time averaged locations of 1000 vortices at $\Lambda = 0.045$ on a slice perpendicular to the z-direction and then averaged over many slices along the thickness of the vortex system; red regions represent higher vortex density and blue regions are lower vortex density. (a) Triangular lattice of vortices in the pure system. (b) Frozen Bose glass phase with 10% strong columnar pins for one realization of disorder. A vortex, with a delta function density distribution, is trapped at the center of a pin (not shown). The blue region is the region of reduced vortex density from which other vortices are repelled by the trapped vortex.

FIG. 2. A snapshot of vortex positions on the top layer (shown as black dots) and the projections on to the top layer of the vortex line (shown in red). Only a portion of the 1000 vortex system is shown for clarity. (a) For $\Lambda = 0.045$ in the solid phase there are very small excursions of the vortex lines. (b) For $\Lambda = 0.065$ just above the melting transition in the clean system the vortex lines are in a highly entangled liquid phase and the vortex density upon averaging is uniform. (c) For $\Lambda = 0.065$ with 10% pins the system is also melted into a defected entangled liquid. In the portion shown there are 3 pins each trapping one vortex, (isolated black dots), which excludes other vortices around it.

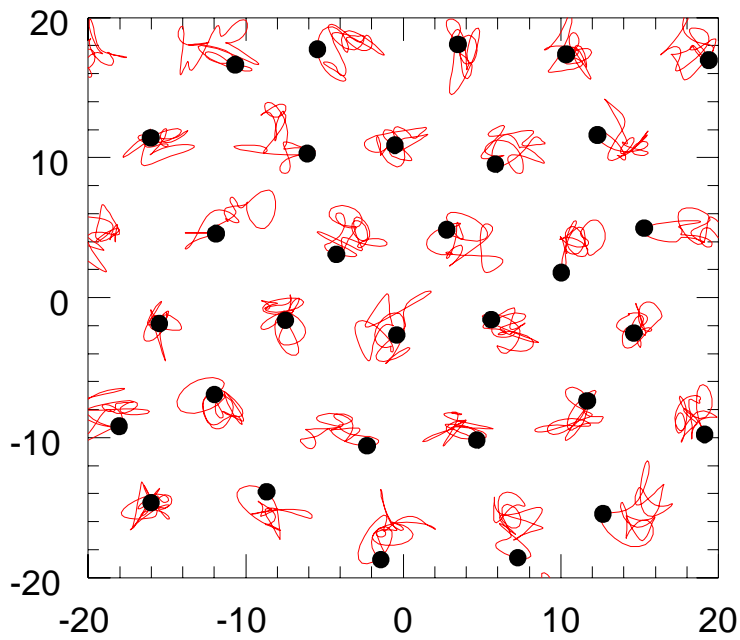
FIG. 3. The structure factor $S(\mathbf{k} = \mathbf{G})$ at the first reciprocal lattice vector of the triangular lattice as a function of Λ for 100 vortices at a density $\rho = 0.02$. The circles show $S(\mathbf{G})$ in the clean system which shows a transition from a crystalline to a liquid phase at $\Lambda \sim 0.064$. The squares show $S(\mathbf{G})$ with 10% columnar pins which shows a much reduced degree of translational order in the Bose glass phase.

FIG. 4. Fraction of non six-fold coordinated sites in the clean and pinned systems. In the clean system the defect density shows a sharp jump across the transition at $\Lambda = 0.064$. In the presence of pins, the topological defect density is higher within the phases and the transition is smoothed out.

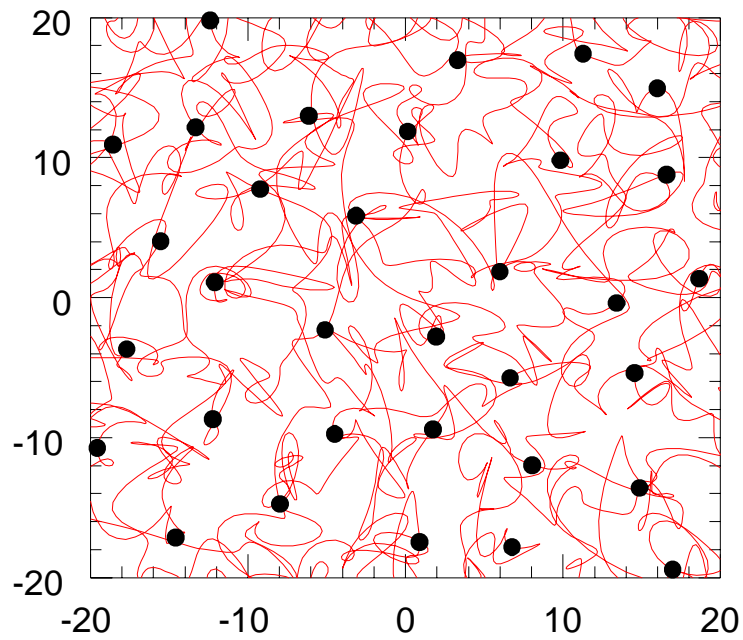
FIG. 5. A 1000 vortex system with 10% columnar pins at $\Lambda = 0.045$ in the Bose glass phase. (a) The structure factor $S(k)$ vs. k showing a much reduced peak from about 250 in the crystal to ~ 6 in the Bose glass phase; but higher than in the liquid with peak height 1.5. (b) The radial positional distribution function $g(r)$ and the orientational correlation function $g_6(r)$. An envelope of the form $\exp(r/\xi)$ can be fit for both $g(r)$ and $g_6(r)$ with $\xi = 13\lambda$ and $\xi = 15\lambda$ respectively. For density $\rho = 0.02$, the inter-vortex separation $a_0 = 7.6\lambda$ so the decay length of the correlations is $\sim 2a_0$ in the Bose glass phase.

This figure "fig1.gif" is available in "gif" format from:

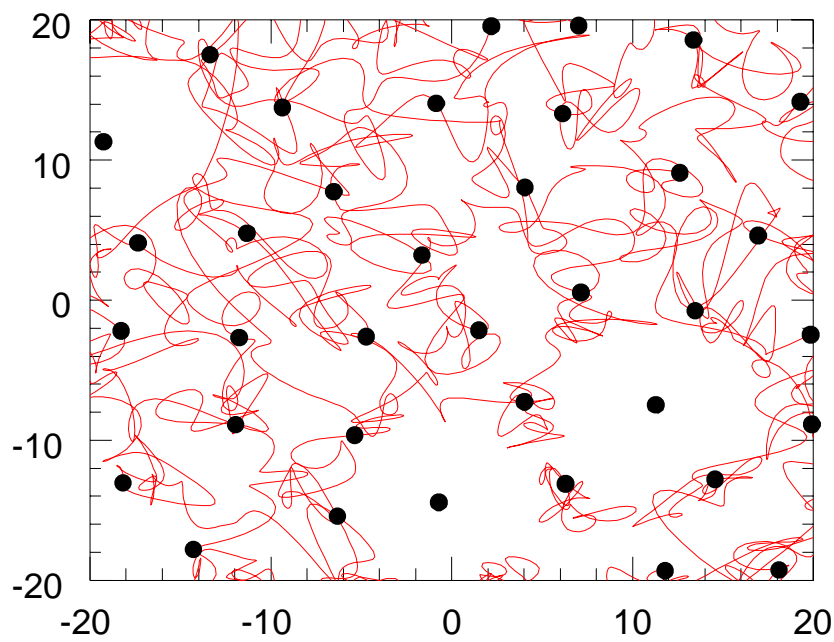
<http://arxiv.org/ps/cond-mat/0008405v1>



$\Lambda=0.045(\text{clean})$



$\Lambda=0.065(\text{clean})$



$\Lambda=0.065(\text{with pins})$

